

Quantitative analysis of the material flow in transitional region during isothermal local loading forming of Ti-alloy rib-web component

Pengfei Gao · He Yang · Xiaoguang Fan

Received: 6 April 2014 / Accepted: 1 August 2014 / Published online: 19 August 2014
© Springer-Verlag London 2014

Abstract The material flow in transitional region plays an important role in the forming quality of transitional region in the isothermal local loading forming of titanium alloy large-scale rib-web component. To study the material flow in transitional region, the finite element (FE) model of transitional region was established based on DEFORM-2D software and validated by physical experiment. Then, a quick and easy method, which can measure the area of different local regions of forged part in DEFORM-2D via user subroutine, was proposed to achieve the quantitative analysis of material flow mechanism. This technique can also be used in the analysis of other forming process, such as the calculation of fill ratio in forging process. The material flow pattern of transitional region during local loading forming was analyzed step by step and compared with integral forming. The results show that the material flow of transitional region during local loading process can be divided into six stages according to the material flow pattern and load-time curve. Twice transverse material flow with opposite directions occurred in the first and second loading steps sequentially, which does not exist in the integral forming. Four characteristic values evaluating the transverse flow of material, which are associated with the formation of defects and their severities, are defined and quantitatively measured at various processing conditions. It is found that decreasing the spacer block thickness and increasing friction both can decrease the four characteristic values, thus weaken the transverse material flow, which are helpful to improve the forming quality in transitional region. However, the transverse flow of material is little affected by the loading speed.

Keywords Isothermal local loading forming · Rib-web component · Transitional region · Material flow

1 Introduction

Large-scale integral components of titanium alloy with thin web and high rib, complex shape (such as bulkhead), having the advantages of light weight and high reliability, are more and more widely applied in aerospace field [1–4]. These components are often used as the key load-bearing structure in some extreme conditions, so high quality of macroscopical forming and fine microstructure is both needed. However, it is difficult to form such components because of the complex shape, hard-to-deform properties of titanium alloy, and high requirement of forming quality. The isothermal local loading forming technique with the advantages of controlling material flow, reducing forming load, improving filling ability, and enlarging the size of component provides a feasible way to form these components [4–6].

However, during isothermal local loading forming, load is applied to part of the billet, and the component is formed by changing loading region. The alternation of loading region results in the loading region, unloading region, and transitional region, as shown in Fig. 1. Transitional region connects the loading region with unloading region and undergoes a passive deformation under the constraints of loading region and unloading region. Some forming defects such as nonuniform microstructure, folding, underfilling, and flow lines disturbance may occur in transitional region due to its complex uneven deformation and material flow. Consequently, the material flow and forming quality of transitional region are the critical concern during local loading forming.

By now, the studies about forming characteristics of transitional region during isothermal local loading mainly focused on the microstructure evolution and processing-

P. Gao (✉) · H. Yang · X. Fan
State Key Laboratory of Solidification Processing, School of
Materials Science and Engineering, Northwestern Polytechnical
University, P.O. Box542, Xi'an 710072, People's Republic of China
e-mail: gp03@126.com

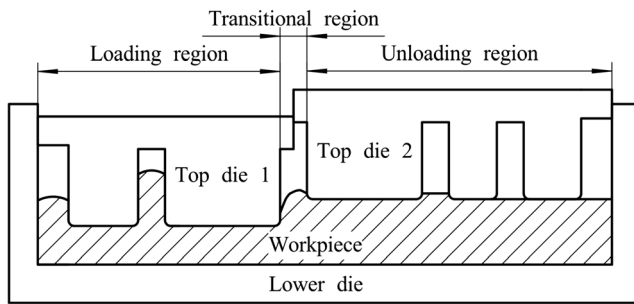


Fig. 1 Illustration of local loading forming

microstructure relationship. Fan et al. [7] studied the microstructure evolution of transitional region in the isothermal local loading forming of titanium alloy by an analogue experiment. Gao et al. [8] quantitatively investigated the effect of processing parameters (deformation temperature, deformation amount, cooling mode, and loading pass) on the microstructure of transitional region under isothermal local loading forming of titanium alloy. These studies supply guidance for the microstructure control of transitional region in isothermal local loading forming of titanium alloy large-scale component. Nevertheless, the investigation focusing on macroscopical forming characteristics of transitional region in local loading forming is still not deep enough. Zhang and Yang [9] investigated the material flow and filling law of ribs in local loading forming of large-scale rib-web component by mathematical models and numerical simulation. Sun et al. [10] studied the influence of die partition on forming quality during local loading forming of H-shaped component using finite element (FE) simulation. They presented that partition at web usually causes burrs or bulges in transitional region, while partition at rib can avoid the occurrence of burrs and bulges and promote the filling of ribs. Sun et al. [11] found that the effect of die partition on the shift of unloading region is a short-range effect during the local loading forming of large-scale component, which mainly concentrated in the region from die partition boundary to the nearest rib of unloading region. As for the material flow in transitional region during local loading forming, Zhang et al. [12] found that there exists some metal flowing from loading area into unloaded area due to local loading characteristic and which may cause some defects in transitional region, such as shift of formed rib, folding, and flow line disturbance. Zhang and Yang [13] further studied the distribution of metal flowing from loading area into unloaded area and suggested that under the partition at rib, the flow-into metal will fill the constraint clearance of unloaded die at first when the unloaded area is unformed, while some of the flow-into metal will fill the cavity of partitioning rib when the unloaded area is formed. However, there is still a lack of in-depth quantitative understanding about the material flow mechanism of transitional region during local loading forming. Moreover, the material flow during forming process determines the forming quality

of transitional region essentially. Therefore, further investigation is required to reveal the material flow mechanism of transitional region during the local loading forming of large-scale rib-web component.

In the present paper, the FE model of transitional region in local loading forming of TA15 alloy large-scale rib-web component was established using DEFORM-2D software and validated by physical experiment. To quantitatively study the material flow mechanism, a convenience method that can measure the area of different regions of workpiece was put forward based on user subroutine of DEFORM-2D. Then, the material flow mechanism of transitional region and its dependence on processing parameters were quantitatively analyzed through FE simulation and four defined characteristic values. The results will deepen our understanding on the material flow mechanism of transitional region and provide basis for controlling the material flow of transitional region in isothermal local loading forming of titanium alloy large-scale rib-web component.

2 FE modeling of transitional region

FE simulation plays an important role in analyzing the deformation characteristics and defects in metal forming, since it can provide a researcher with various forming knowledge such as distribution of stress, strain and velocity, and the evolution of defects during forming process [14–16]. So, FE simulation was also applied to study the material flow of transitional region in this work. As mentioned in Sect. 1, in local loading forming of rib-web components, partition at rib is preferred in comparison with partition at web considering the filling of ribs and prevention of burrs. Besides, the effect of loading area on the shift of unloading region is a short-range effect, which mainly affects the region from the die partition boundary to the nearest rib of unloading region. Therefore, based on the structural features of large-scale rib-web component, the transitional region eigen model partitioning at rib and containing the nearest rib to partition rib was extracted, and whose FE model was established under DEFORM-2D environment, as shown in Fig. 2. Since the metal flow along direction perpendicular to die partition boundary is main deformation, the influence of tangential deformation is neglected, and the deformation in transitional region is simplified as a plane strain problem in this work. Same simplification was also conducted in previous analysis on the deformation behavior of large-scale rib-web components and was confirmed to be reasonable [17, 18]. The typical local loading process has two loading steps, which is implemented as follows. In the first loading step, a spacer block is implanted between top die 1 and top die bed with top die 1 protuberant, which makes the billet under top die 1 deforms first. In the second loading step, the spacer block is removed with top die

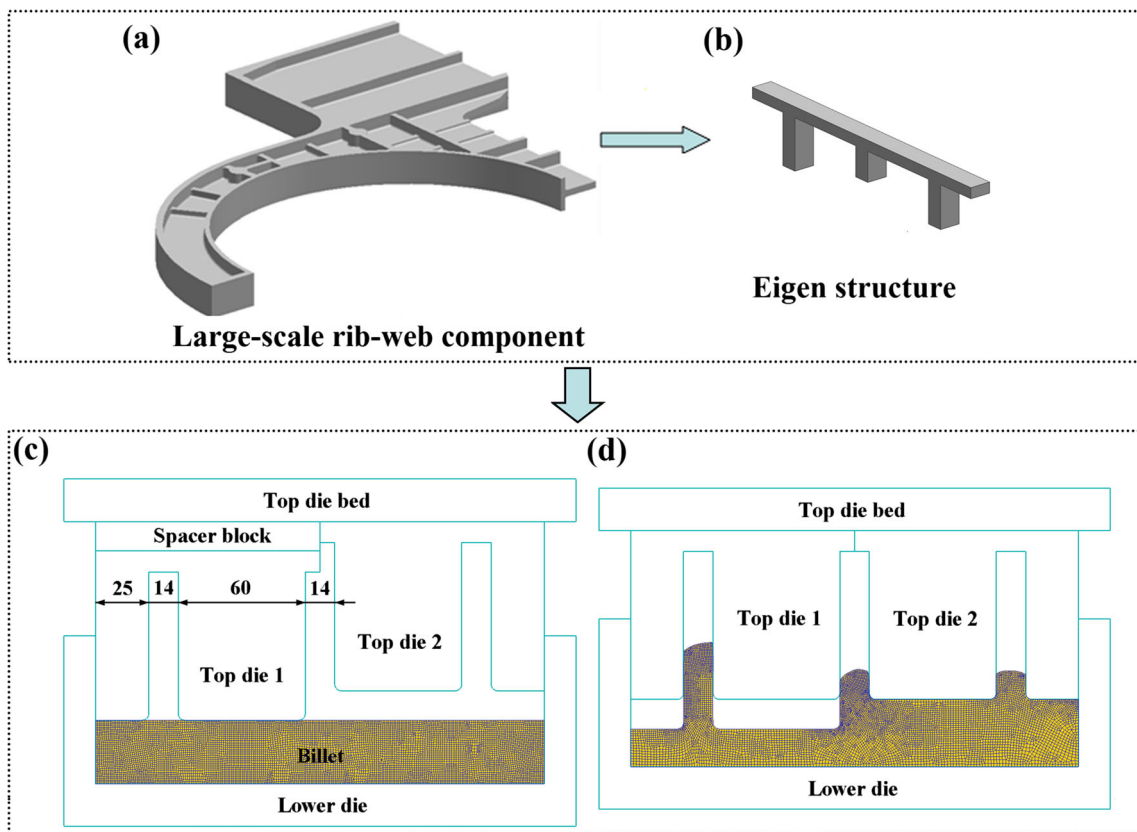


Fig. 2 Sketch of the FE model of transitional region in local loading forming of large-scale component. **a** Large-scale rib-web component. **b** Eigen structure. **c** The first loading-step of transitional region eigen model. **d** The second loading step of transitional region eigen model

1 and top die 2 being at the same level. The geometry dimensions of top dies in this work are shown in Fig. 2c. Top die 1 and top die 2 are symmetrical, and the fillet radius is 3 mm. As the isothermal local loading is performed under high temperature and low loading speed, the thermal events are neglected in FE model. The Von Mises yielding criteria and shear friction model are employed. The local refined meshing and automatic remeshing techniques provided by DEFORM-2D software are used to avoid meshing-induced singularity, which have also been adopted by Zhang et al. [18].

Physical experiment has been extensively used in the field of metal forming to perform experimental observations instead of real tests due to its advantages of reduction in forming load and requirement to forming machine, easy observation of the material flow pattern, and low cost. Previous study [19] suggested that the flow behavior of lead at room temperature is similar to that of titanium alloy at elevated temperatures. Moreover, the physical experiment taking lead as model material has been successfully used to investigate the forming characteristics of titanium alloy T-shaped and double T-shaped components during isothermal local loading forming [11, 17]. Thus, the physical experiment using lead was conducted to validate the FE model of transitional region during local loading forming. The material of die for experiment is

steel 1045. The physical experimental is performed at a 60-t hydraulic press at room temperature. The desired billet size is 212×20×30 mm. To observe the material flow in local loading forming, the billet was cut into two symmetrical parts, and the meshes, 3 mm in width, were marked in cross section of lead sample. As the meshes would undergo large deformation and become indistinct at larger reduction amount, a smaller reduction amount of 6 mm was conducted in the experiment. The main processing parameters are shown in Table 1. After

Table 1 Main parameters in the physical experiment and FE model

	Experiment	FE-lead	FE-TA15
Material of billet	Lead	Lead	TA15
Deformation temperature (°C)	Room temperature	20	950
Friction factor (<i>m</i>)	Consistent grease	0.4	0.4
Loading speed (mm/s)	–	0.1	0.1
Loading pass	1	1	1
Reduction amount (mm)	6	6	6
Thickness of spacer block (mm)	6	6	6

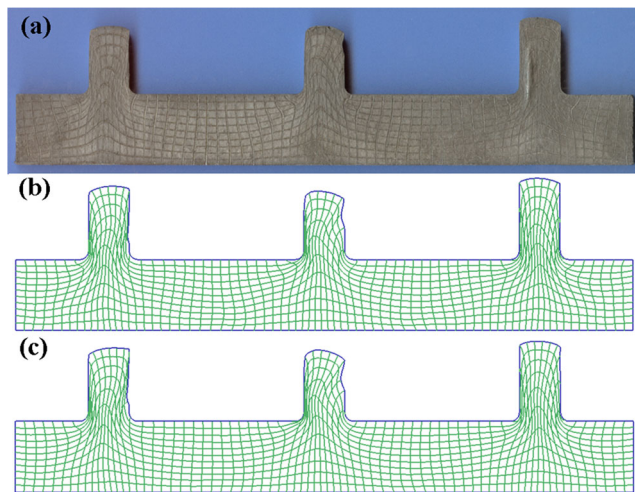


Fig. 3 Local loading formed sample: **a** experimental result, **b** FE simulation result with material of lead (FE-lead), and **c** FE simulation result with material of TA15 alloy (FE-TA15)

deformation, the flash was removed, and the formed sample was scanned by scanner, as shown in Fig. 3a.

The corresponding FE models of physical experiment were established with material models of lead from [17] (Eq. (1)) and TA15 alloy from Shen [20] using the same modeling techniques above, respectively.

$$\sigma = 30.20826\varepsilon^{0.11847} \quad (1)$$

Considering the volume loss in experiment (V_l), the height of billet (H_b) in FE model is set as 29.415 mm, which is calculated by the following equation:

$$H_b = 30 - V_l / 20 / 212 \quad (2)$$

The volume loss consists of two parts as explained below. The volume loss caused by assembling clearance (V_s) could be estimated by Eq. (3).

$$\begin{aligned} V_s &= 212 \times 20 \times 30 - 211.85 \times 19.75 \times 29.9 \\ &= 2097.279 \text{mm}^3 \end{aligned} \quad (3)$$

In addition, the flash produced in two loading steps also gives rise to the volume loss. This part of volume loss (V_f) was measured about 381.164mm^3 . So, the total volume loss in experiment (V_l), the summation of V_s and V_f , is 2478.443mm^3 . The other main parameters in FE model are listed in Table 1. Figure 3b shows the simulation result of FE model with material of lead. It can be found that the shape and meshes of simulated sample both agree well with the experimental results (Fig. 3a). Besides, the quantitative comparisons between the simulation result of FE model with lead and experimental result are carried out on the heights of three ribs,

as given in Table 2. The comparison results show that the average and maximum relative errors between experimental and simulation results are 4.06 and 6.68 %, respectively. Figure 3c shows the simulation result of FE model with material of TA15 alloy, which is very close to the physical experiment result and simulation result of FE model with material of lead. The overall comparisons between FE simulation and experimental results suggest that the established FE model of TA15 alloy above is reliable and applicable to study the material flow in transitional region during isothermal local loading forming of TA15 alloy large-scale rib-web component.

3 Measurement method for quantity of material in prescribed local region of workpiece

In order to quantitatively analyze the material flow in transitional region during local loading forming, it is necessary to measure the quantity of material in different local regions of workpiece at different times. In this work, the quantity of material of a local region means its area, which is measured based on the FE simulation result.

When calculating the fill ratio of final die cavity in forging process, it is also required to measure the area of forged part [21–23]. Abdullah et al. [22, 23] investigated the underfilling defect in cold forging of pinhead through FE simulation by DEFORM-2D. They measured the area of forged part as following: First, capture the image of forged pinhead in DEFORM-2D to determine the geometry of the part and then calculate the area of forged part based on the captured image by a program developed using Matlab software. Besides the Matlab software, the area of forged part can also be measured by image quantitative analysis software, such as Image-Pro Plus software, based on the part image. However, these two methods both need image acquisition, spatial calibration, and boundary identification, which are laborious and error-prone.

In the present work, a quick and easy way was proposed to measure the area of different local regions of part in DEFORM-2D via user subroutine. The calculation process of this method is given below: (1) Calculate the area of each element. The element in DEFORM-2D is quadrilateral, and its four corner coordinates are available in the user subroutine (USRMSH). In addition, four corners are stored sequentially,

Table 2 Heights of three ribs in the experiment and FE simulation results

	Left rib/mm	Middle rib/mm	Right rib/mm
Experiment	23.52	23.31	26.33
FE-lead model	25.09	23.36	27.72
Error/%	6.68	0.21	5.28

so the area of each element can be obtained by calculating the area of two triangles according to plan geometry (Fig. 4). (2) Define the boundaries of concerned regions by mathematical expression. In this work, the concerned regions are all divided by lines parallel to vertical axis, as shown in Fig. 4 (red lines). So, the abscissa values of these dividing lines are passed into user subroutine through user defined data (USRDEF) field in preprocessor. (3) Judge the positional relation between each element and concerned regions. Three situations exist here: (a) element locates in the concerned region totally, (b) element does not locate in the concerned region, and (c) region boundary cuts through the element with only part of element locating in the concerned region. (4) Calculate the area attribute values of each element for different regions according to their positional relations and store them as user defined element state variables. The area attribute values of element for a concerned region are the element area, 0, and area of the partial element located in concerned region for positional situation a, b, and c, respectively. In situation c, area of the partial element located in concerned region is calculated approximately, as shown in Fig. 4. (5) Last, the area of each region at each step can be obtained by summing the corresponding area attribute value of all elements.

4 Results and discussion

4.1 Description of the material flow in transitional region

With the aid of FE simulation, material flow mechanism of transitional region is analyzed through the evolutions of velocity vector field and part shape during forming process in this section. Processing parameters of the typical sample

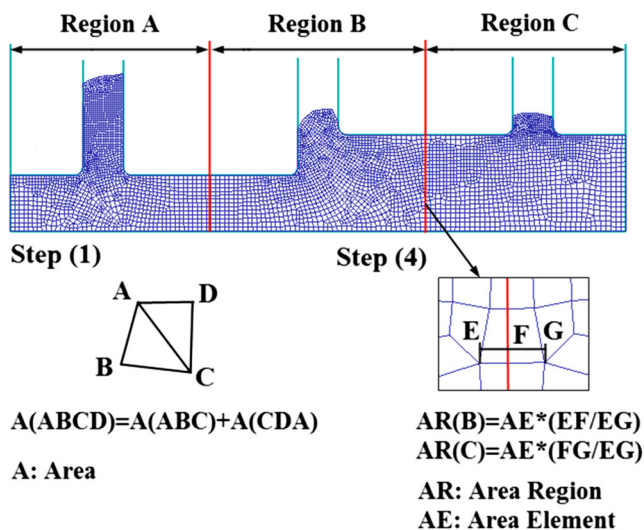


Fig. 4 Illustration of the calculation of different regions areas in DEFORM-2D

analyzed here are as follows. The billet height is 30 mm, reduction amount is 12 mm, and spacer block thickness is 14 mm. The loading speed is 0.5 mm/s, deformation temperature is 950 °C, and friction coefficient is 0.3.

According to the load-time curve (Fig. 5) and variation of velocity field during forming process, the whole local loading process can be divided into six forming stages with three stages in each loading step, as shown in Fig. 5. The representative velocity field of each forming stage and the workpiece after each stage are shown in Fig. 6. For the first loading step, in stage 1, top die 1 press the workpiece, while top die 2 does not contact the workpiece. As punch descends, the materials under top die 1 fill into the left rib and move right at the same time due to the lower resistances in unloading region. With the increase of punch stroke, more and more material flow to unloading region and lead to the haunch-up of workpiece in unloading region. When top die 2 contacts the material, stage 2 begins. In stage 2, the constraint of top die 2 to workpiece occurs and increases with the contact area (indicted by yellow dots in Fig. 6). As a result, the rightward transverse flow of material is suppressed to some extent, and a neural layer emerges between the left rib and middle rib. Yet, material on the right side of neural layer still has a tendency to flow right. Stage 2 ends until top die 2 contacts the workpiece totally. The left rib is filled continually, and the middle and right ribs are both filled slightly in this stage. In stage 3, top die 1 and top die 2 press the workpiece simultaneously, and the material flow pattern is similar to that of integral forming (Fig. 7). Besides the neural layer between the left and middle ribs generated in stage 2, a new neural layer emerges between the middle rib and right rib. Each rib is filled from both sides in this stage, which is a preferable filling style in the forming of rib-web component. Stage 3 lasts to the end of first loading step with a shorter period.

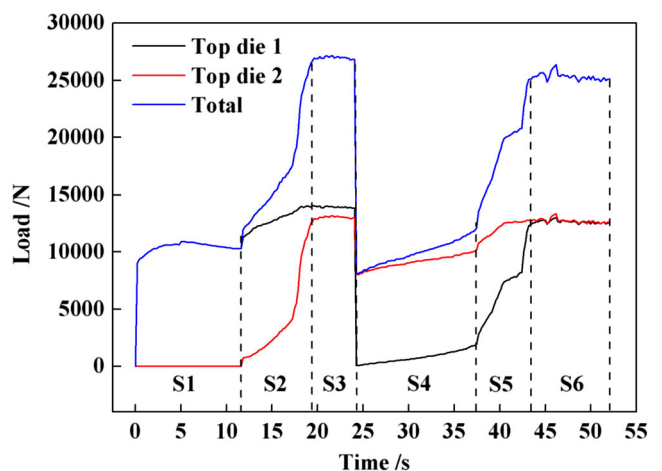
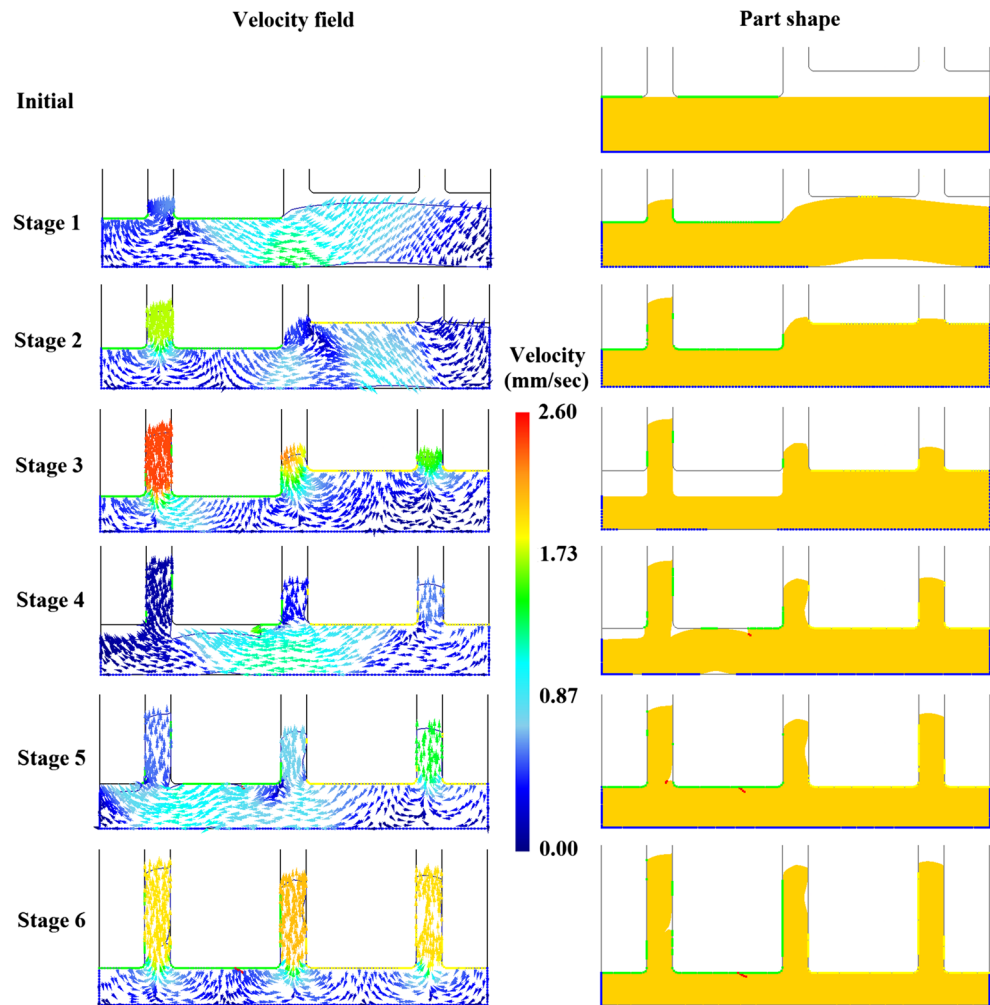


Fig. 5 Load-time curve in the local loading forming

Fig. 6 The representative material flow patterns and part shapes at different forming stages



For the second loading step, in stage 4, the workpiece is mainly pressed by top die 2. The materials under top die 2 fill into the right and middle ribs and move left at the same time due to the gap between top die 1 and the workpiece. As a result, a step is formed between the left rib and middle rib, as shown in Fig. 6. On the other hand, the faster leftward transverse flow of material under the middle rib drives the material in rib root move left with its upward filling to the rib, which generates a cavum at the right side of the middle rib. As punch descends, more and more material flow left leading to the haunch-up of the formed web in first-loading region and then folding developed from the step. When the warped web contacts top die 1, stage 5 begins. Due to the increase of resistance in the first-loading region, the leftward transverse flow of material is suppressed to some extent, and a neural layer emerges between the right rib and middle rib. While, the material on the left side of neural layer still has a tendency to flow left. In this stage, the formed left rib shifts to left a little, and a V-shaped cavum is then formed at its root because of the leftward transverse flow of the material under the left rib. The gap between top die 1 and workpiece reduces gradually until

disappear; the long-range transverse flow of web material get weaken gradually and stop due to the increase of resistance. In stages 4 and 5, the right rib and middle rib are filled continually, but the left rib is filled little. In the following stage (stage 6), two neural layers exist between the adjacent two ribs, and each rib is filled from both sides as that in stage 3. In this stage, the V-shaped cavum at the left rib and the curved cavum at the middle rib both move up with the filling of ribs.

To analyze the special features of material flow in local loading, the material flow pattern of integral forming is given as a comparison in Fig. 7. The material flow pattern of integral

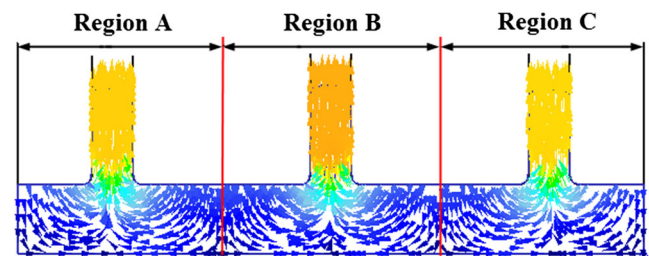


Fig. 7 Material flow pattern in the integral forming

forming varies little through the whole forming process. Two neural layers (red lines in Fig. 7) exist between the adjacent two ribs, and three ribs are both filled from both sides. The workpiece is divided into three regions by two neural layers, and there is no material flow among three regions each other, as shown in Fig. 7. However, in local loading forming, the material flow between adjacent regions occurs and varies with forming stage. This is the greatest difference on material flow between the local loading forming and integral forming. The changes of material quantity in three regions (Fig. 7) with forming stage are measured in local loading forming and shown in Fig. 8.

From Fig. 8, it can be found that the quantity of material in region A decreases first in stages 1 and 2 and then increases till stage 5, yet, it varies little in stage 6. The quantity of material in region B shows a descending trend basically with forming stage, but the decreasing amount is small. On the other hand, the material quantity in region C increases first in stages 1 and 2 and then decreases till stage 5, yet, it varies little in stage 6. The changes of material quantity in three regions suggest that the material in transitional region underwent a rightward transverse flow process first and then a leftward transverse flow process during the local loading forming. This is in accordance with the analysis results obtained by material flow pattern during forming process. For the final quantities of material in three regions, it can be seen that the quantities of material in regions A and C increase slightly than the initial values, while those in region B decrease a little than the initial value. The changes are all very small and present little effect on the filling height of each rib. But, the reciprocating transverse flow of material may lead to forming defects. As analysis above, the folding defect and cavums in the left and middle ribs generate with the leftward flow of material in second loading step. It can be inferred that the quantities of

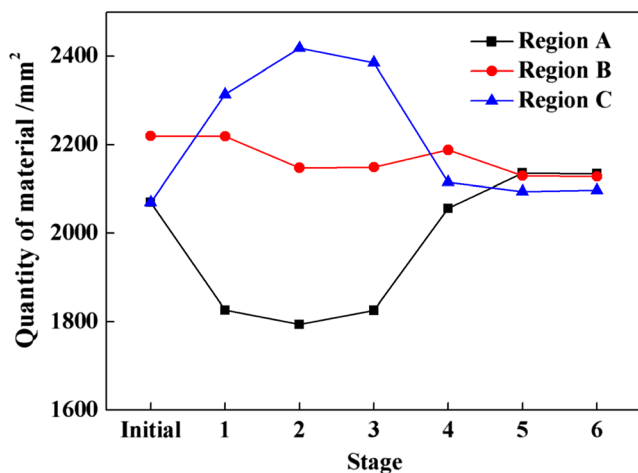


Fig. 8 Changes of material quantity in different regions with forming stage in local loading forming

material flowed into regions D, E, F, and G (Fig. 9) during the leftward flow process in second loading step, i.e., stages 4 and 5, determine the severities of defects. The quantities of material flowed into regions D and E are related to the cavum in the left rib, and the quantities of material flowed into regions F and G are related to the folding defect and cavum in the middle rib. More transverse material flow leads to more serious forming defects. In the present work, Q_D , Q_F , Q_D/Q_E , and Q_F/Q_G (where Q_D , Q_E , Q_F , and Q_G represent the quantity of material flowed into regions D, E, F, and G, respectively) are taken as four characters to evaluate the material flow in transitional region. Considering the control of forming defects, the effects of processing conditions on these four characters of material flow were studied quantitatively in Sect. 4.2.

4.2 Effect of processing conditions on the characters of material flow

In this study, the effects of processing conditions on material flow are studied using single factorial experiments. Three processing parameters were studied: thickness of spacer block (H_{sb}), friction coefficient (m), and loading speed (v). Among, thickness of spacer block is determined according to reduction amount (L) and must satisfy the constraint that $H_{sb} \geq L$. Variable values are listed in Table 3, where the values in bold are default values adopted in simulations when investigating the effect of other parameters on defects. The billet height and reduction amount of these samples are all 30 and 12 mm, respectively, and these samples are all deformed at 950 °C.

Figure 10 shows the variations of material flow characters with different processing parameters. It can be seen from Fig. 10a that decreasing H_{sb} could decrease Q_F and Q_F/Q_G , which can suppress the folding defect and cavum in the middle rib. On the other hand, Q_D decreases with the decrease of H_{sb} , while Q_D/Q_E decreases obviously first and then changes little with the descending of H_{sb} . Thus, smaller H_{sb} is also beneficial to suppress the cavum in the left rib. From Fig. 10b, it can be found that four characters Q_D , Q_F , Q_D/Q_E , and Q_F/Q_G

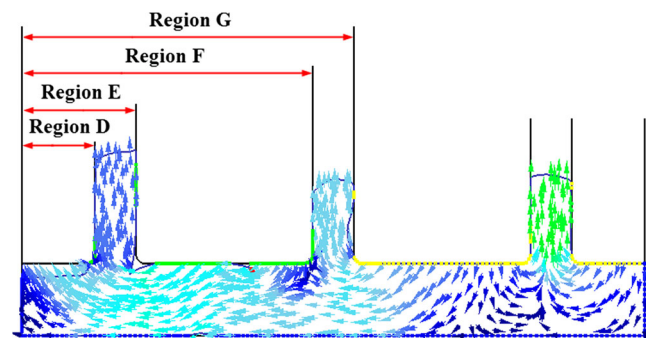


Fig. 9 Illustration of regions D, E, F, and G

Table 3 Parameter values for FE simulations of local loading forming

Processing parameters	Value 1	Value 2	Value 3	Value 4	Value 5
Spacer block thickness H_{sb} (mm)	L (12)	$L+1$ (13)	$L+2$ (14)	$L+3$ (15)	$L+4$ (16)
Friction coefficient m	0.1	0.2	0.3	0.4	0.5
Loading speed v (mm/s)	0.1	0.3	0.5	0.7	0.9

all show descending tendency with the increase of friction coefficient. It indicates that increasing friction between die and workpiece could suppress the transverse flow of material, thus promoting the forming quality. From Fig. 10c, it can be seen that the loading speed has little effect on these four characters of material flow.

Above, it can be concluded that decreasing H_{sb} and increasing friction could suppress the transverse flow of material, which are helpful to forming quality. But, loading speed has little effect on the transverse flow of material in transitional region in this work. The relationship between material flow characters and forming defects and the dependence of forming defects on processing conditions will be studied systematically in the future work.

5 Conclusions

In this work, the FE model of transitional region in local loading forming of TA15 alloy large-scale rib-web component was established using DEFORM-2D software and validated by physical experiment, through which the material flow mechanism and its dependence on the processing conditions were investigated quantitatively. From this work, the following conclusions can be drawn:

1. A quick and easy way to measure the area of different local regions of forged part in DEFORM-2D via user subroutine was proposed so as to achieve a quantitative analysis on the material flow mechanism. This technique

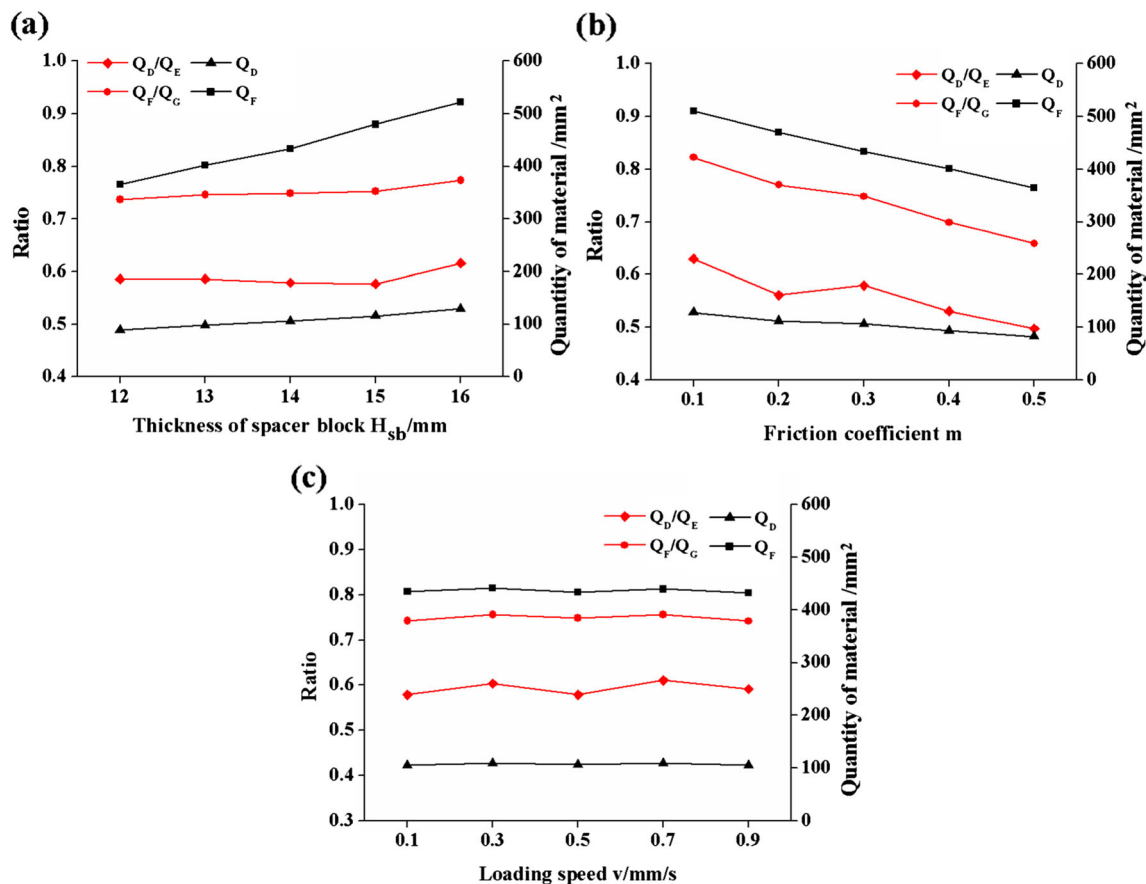


Fig. 10 Variations of characters of material flow with different processing parameters: **a** thickness of spacer block (H_{sb}), **b** friction coefficient (m), and **c** loading speed (v)

can also be used in analysis of other forming process, such as the calculation of fill ratio in forging process.

2. According to the variation of load and velocity vector field during forming process, the whole local loading process can be divided into six forming stages, with each loading step segmented into three stages. Twice long-range transverse flow of material with opposite directions occurred in the first loading step and second loading step sequentially, which does not exist in integral forming. It is the reciprocating transverse flow of material that may lead to forming defects.
3. Four characters representing the transverse flow of material are defined, which may determine the formation of defects and their severities. It is found that for a certain reduction amount, decreasing the spacer block thickness and increasing the friction both can weaken the transverse flow of material, resulting in smaller characters, which are helpful to control the defects in transitional region. However, the transverse flow of material is little affected by the loading speed. The relationship between these four characters and forming defects and the dependence of forming defects on processing conditions should be studied systematically in the future work.

Acknowledgments The authors would like to gratefully acknowledge the supports of the National Natural Science Foundation of China for Key Program (No. 50935007), National Basic Research Program of China (No. 2010CB731701), National Natural Science Foundation of China (No. 51205317), 111 Project (B08040), and Excellent Doctorate Foundation of Northwestern Polytechnical University.

References

1. Shen G, Furrer D (2000) Manufacturing of aerospace forgings. *J Mater Process Technol* 98:189–195
2. Zhang DW, Yang H (2013) Preform design for large-scale bulkhead of TA15 titanium alloy based on local loading features. *Int J Adv Manuf Technol* 67:2551–2562
3. Sun ZC, Yang H, Sun NG (2012) Effects of parameters on inhomogeneous deformation and damage in isothermal local loading forming of Ti-alloy component. *J Mater Eng Perform* 21(3):313–323
4. Sun ZC, Yang H (2009) Microstructure and mechanical properties of TA15 titanium alloy under multi-step local loading forming. *Mater Sci Eng A* 523(1–2):184–192
5. Fan XG, Yang H, Sun ZC, Zhang DW (2010) Effect of deformation inhomogeneity on the microstructure and mechanical properties of large-scale rib-web component of titanium alloy under local loading forming. *Mater Sci Eng A* 527:5391–5399
6. Sun ZC, Yang H (2009) Forming quality of titanium alloy large scale integral components isothermal local loading. *Arab J Sci Eng* 34(1C):35–45
7. Fan XG, Gao PF, Yang H (2011) Microstructure evolution of the transitional region in isothermal local loading of TA15 titanium alloy. *Mater Sci Eng A* 528(6):2694–2703
8. Gao PF, Yang H, Fan XG (2011) Quantitative analysis of the microstructure of transitional region under multi-heat isothermal local loading forming of TA15 titanium alloy. *Mater Des* 32(4):2012–2020
9. Zhang DW, Yang H (2013) Metal flow characteristics of local loading forming process for rib-web component with unequal-thickness billet. *Int J Adv Manuf Technol* 68:1949–1965
10. Sun Z, Yang H, Li Z (2009) H-Shaped component isothermal local loading forming of TA15 titanium alloy. *Rare Metal Mater Eng* 38(11):1904–1909
11. Sun ZC, Yang H, Sun NG (2009) Simulation on local loading partition during titanium bulkhead isothermal forming process. *J Plast Eng* 16(1):138–143 (in Chinese)
12. Zhang DW, Yang H, Sun ZC, Fan XG (2011) Deformation behavior under die partitioning boundary during titanium alloy large-scale rib-web component forming by isothermal local loading. *Proceedings of the 12th World Conference on Titanium*. Science Press, Beijing, p 328
13. Zhang DW, Yang H (2014) Distribution of metal flowing into unloaded area in the local loading process of titanium alloy rib-web component. *Rare Metal Mater Eng* 43(2):296–300
14. Zhou J, Wang F, Wang M, Xu W (2011) Study on forming defects in the rolling process of large aluminum alloy ring via adaptive controlled simulation. *Int J Adv Manuf Technol* 55:95–106
15. Saxena RK, Dixit PM (2009) Finite element simulation of earing defect in deep drawing. *Int J Adv Manuf Technol* 45:219–233
16. Wang JL, Fu MW, Ran JQ (2013) Analysis and avoidance of flow-induced defects in meso-forming process: simulation and experiment. *Int J Adv Manuf Technol* 68:1551–1564
17. Zhang DW, Yang H, Sun ZC (2010) Analysis of local loading forming for titanium-alloy T-shaped components using slab method. *J Mater Process Technol* 210:258–266
18. Zhang DW, Yang H, Sun ZC, Fan XG (2012) Deformation behavior of variable-thickness region of billet in rib-web component isothermal local loading process. *Int J Adv Manuf Technol* 63(1–4):1–12
19. Dutta A, Rao AV (1997) Simulation of isothermal forging of compressor disc by combined numerical and physical modeling techniques. *J Mater Process Technol* 72(3):392–395
20. Shen CW (2007) Research on material constitution models of TA15 and TC11 titanium alloys in hot deformation process. Master Thesis, Northwestern Polytechnical University
21. Tang YC, Zhou XH, Chen J (2008) Preform tool shape optimization and redesign based on neural network response surface methodology. *Finite Elem Anal Des* 44:462–471
22. Abdullah AB, Sapuan SM, Samad Z, Khaleed HMT, Aziz NA (2012) Prediction of geometric defects in the cold embossing of AA6061 aluminum alloy by finite element analysis. *Sci Res Essays* 7(15):1630–1638
23. Abdullah AB, Sapuan SM, Samad Z, Khaleed HMT, Aziz NA (2013) Numerical investigation of geometrical defect in cold forging of an AUV blade pin head. *J Manuf Proc* 15(1):141–150